Calorimetric and neutron diffraction studies of the commensurate - incommensurate spin-density-wave phase transition of Cr+0.3 at.% Ru alloy

1996 J. Phys.: Condens. Matter 8 7837

(http://iopscience.iop.org/0953-8984/8/42/003)

J. Phys.: Condens. Matter **8** (1996) 7837–7846. Printed in the UK

Calorimetric and neutron diffraction studies of the commensurate–incommensurate spin-density-wave phase transition of Cr + 0.3 at.% Ru alloy

R S Eccleston†, M Hagen†, Ll Mañosa‡, G A Saunders§ and H L Alberts‖

† ISIS Facility, Rutherford Appleton Laboratory, Chilton, Didcot, Oxon, UK

‡ Departament d'Estructura i Constituents de la Matèria, Facultat de Física, Universitat de Barcelona, Diagonal 645, 08028 Barcelona, Catalonia, Spain

§ School of Physics, University of Bath, Claverton Down, Bath, UK

‖ Department of Physics, Rand Afrikaans University, PO Box 524, Johannesburg 2000, South Africa

Received 16 May 1996, in final form 16 August 1996

Abstract. Calorimetric and time-of-flight neutron diffraction experiments are used to establish thermodynamic and structural features of a Cr + 0.3 at.%Ru alloy crystal as it undergoes a commensurate-to-incommensurate spin-density-wave (CDSW–ICDSW) phase transition. Both methods confirm the first-order character of the transition. The calorimetric measurements made at the CSDW–ICSDW transition, using a differential scanning microcalorimeter, show that the latent heat $|\Delta H|$ (=5.6 ± 0.5 J mol^{-1}) and entropy $|\Delta S|$ (=0.023 ± 0.003 J mol^{-1} K^{-1}) changes at the transition are small: the transition is only weakly first order. The difference between the specific heat C_P^I of the incommensurate phase and that, C_P^C, of the commensurate phase is determined as 0.20 ± 0.14 J K^{-1} mol^{-1}. In the neutron diffraction experiments the thermal evolution of the intensities and positions of the commensurate and the incommensurate peaks have been monitored in the region of the transition. There is a temperature range of approximately 28 K in which the commensurate and the incommensurate peaks coexist. This coexistence of the two phases is consistent with a broad anomaly observed in the specific heat.

1. Introduction

In its antiferromagnetic state below a Néel temperature of 312 K pure chromium exhibits a transverse spin-density-wave (SDW) structure, which is incommensurate with the bcc lattice [1–5]. The large amplitude of the static SDW is related to a special geometric feature of the Fermi surface, which allows nesting between electron and hole pockets having similar shapes [2]. These are connected by a nesting vector directed along an [001] axis, nearly but not quite equal to the SDW wavevector: the wavevector $\boldsymbol{Q}$ (=$(2\pi/a)(1-\delta)$) of the SDW, where δ is the incommensurability parameter, is incommensurate with the lattice spacing. Nesting between the electron and hole Fermi surface sheets, which stabilizes the SDW, can be improved by dilute alloying with a metallic element, such as Ru, having more outer electrons than Cr to increase the electron-to-atom (e/a) ratio [5, 6]. This raises the Fermi level, increasing the size of the electron Fermi surface, while reducing that of the holes. For an e/a ratio only slightly larger than the value of six for Cr, the antiferromagnetic SDW periodicity jumps from an incommensurate (I) to a commensurate (C) state [6, 7]. The Cr alloys containing Ru in the region of 1 to 5 at.% exhibit a commensurate spin-density-wave (CSDW) structure below the Néel temperature down to 4 K [5, 8, 9]. In

0953-8984/96/427837+10$19.50

alloys having an even lower Ru concentration the CSDW structure undergoes a transition to the incommensurate SDW (ICSDW) state as the temperature is reduced. In fact the ISDW phase is found in most dilute Cr alloys to be the stable low-temperature phase while the CSDW phase is the stable one at high temperatures [5]. There are several theoretical models to explain this [5]; a qualitative explanation has been based on the model in which at low temperatures a large area of Fermi surface is annihilated, stabilizing the incommensurate SDW state, while at high temperatures only a small area is affected, and so the commensurate structure is stable [6].

The nature and driving mechanism of the CSDW–ICSDW transition at the atomic level are not yet firmly established. Cankurtaran *et al* [10] have made a detailed ultrasonic study of this transition in an alloy with a concentration Cr + 0.3 at.% Ru (e/a ratio 6.006) chosen because the transition occurs on cooling at the readily accessible temperature of about 250 K. Large differences were observed between the elastic and non-linear acoustic properties of the commensurate SDW and the incommensurate SDW phases. Both phases, especially the commensurate SDW one, exhibit particularly interesting non-linear acoustic behaviour. There is a strong magnetoelastic interaction leading to a softening of the long-wavelength longitudinal acoustic phonons under pressure. The velocities of longitudinal and shear modes show a large and steep increase at the transition temperature T_{CI} from the CSDW to the ICSDW (which takes place on cooling) and a corresponding decrease at T_{IC} (on warming). There is a difference between the T_{CI} and T_{IC} measured during the cooling and warming cycles, a hysteresis indicating that the CSDW-to-ICSDW transition is first order in character. The ultrasonic measurements of the pressure dependence of the transition temperature enabled determination of the latent heat, using the Clausius–Clapeyron equation, and in turn the entropy change at the transition for the Cr + 0.3 at.% Ru alloy. However, this is an indirect method, which suffers from cumulative error from the measurements of the pressure derivative and the small volume change at the transition; in addition for transitions having a temperature spread this approach has the difficulty of definition of an actual transition temperature and its pressure dependence. By contrast, calorimetry is a direct technique for obtaining latent heat and entropy changes, provided that the temperature is continuously monitored. Calorimetry provides additional thermodynamic information in that the difference in specific heat between the two phases can be determined. To achieve this, calorimetric measurements have now been made at the CSDW–ICSDW transition in the Cr + 0.3 at.% Ru alloy crystal using a sensitive differential scanning calorimeter.

Another approach used to extend understanding of the nature of the CSDW–ICSDW transition has been to make a more detailed study of the structural changes which happen in its vicinity. Recently Boshoff *et al* [11] have conducted an ultrasonic and neutron diffraction study of a Cr + 0.3 at.% Ru single crystal. Their ultrasonic data are in reasonable agreement with those of Cankurtaran *et al* [10], and their neutron scattering data suggest that in the ICSDW phase, the magnetic structure is the same as that in pure chromium. As an integral part of the present work, the structure and excitations of this alloy have been followed using time-of-flight neutron scattering techniques, paying particular attention to developing further knowledge of the way in which the commensurate-to-incommensurate structural changes proceed as the alloy approaches the vicinity of and then goes through the CSDW–ICSDW transition.

2. Experimental procedures

The Cr + 0.3 at.% Ru alloy on which calorimetric measurements were made was a piece cut from the same single crystal as was used for the earlier ultrasonic experiments [10].

Electron microprobe analysis showed that its composition was 0.28 ± 0.02 at.% Ru and was homogeneous within the instrumental resolution. When single crystals are grown from the melt of any binary metal alloy in which the solidus and liquidus on the phase diagram do not coincide (this is true of almost all such systems), there is inevitably a small concentration gradient, of magnitude dependent upon the solidus–liquidus separation, along the specimen and also a tendency towards an inhomogeneous distribution of solute atoms. Such compositional variations could not be discerned in our analysis to within ± 0.02 at.% Ru but that does not preclude their existence to that level.

A particularly sensitive differential scanning microcalorimeter, specifically designed to investigate solid–solid phase transitions [12, 13] has been needed to make the measurements. The system is computer controlled and acquires simultaneously the thermal power $(\mathrm{d}Q/\mathrm{d}t)$ and the temperature, at a typical reading rate of 0.5 Hz. The latent heat is obtained by integrating the calorimetric curve $(\mathrm{d}Q/\mathrm{d}t)$ after correction from the base-line:

$$\Delta H = \int_{T_s}^{T_f} \left(\frac{\mathrm{d}Q}{\mathrm{d}t}\right) \dot{T}^{-1}\, \mathrm{d}T \tag{1}$$

where $\dot{T}$ is the heating/cooling rate and T_s and T_f are the temperatures at the start and finish respectively of the transformation. The entropy change of the transition can be computed from

$$\Delta S = \int_{T_s}^{T_f} \left(\frac{1}{T}\right)\left(\frac{\mathrm{d}Q}{\mathrm{d}t}\right) \dot{T}^{-1}\, \mathrm{d}T. \tag{2}$$

Notice that $\mathrm{d}Q/\mathrm{d}T = (\mathrm{d}Q/\mathrm{d}t)\dot{T}^{-1}$ is proportional to the difference in specific heat between the specimen and a reference sample; thus, differences in the specific heat between the different phases of the sample under study appear as changes in the calorimetric curve.

The neutron diffraction measurements were carried out on another single crystal of Cr + 0.3 at.% Ru grown from high-purity starting materials by a floating-zone technique using rf heating. This crystal was also analysed by an electron microprobe analysis: its composition was also 0.28 ± 0.02 at.% Ru and it too was homogeneous within the instrumental resolution. The crystal had cylindrical shape, 6 mm in diameter and 20 mm long, with the [100] axis approximately 10° from the cylindrical axis. The sample was mounted in a closed-cycle refrigerator with a $[1\bar{1}0]$ axis vertical so that reflections of the form (hhl) could be observed in the horizontal scattering plane. The neutron scattering measurements were carried out using the PRISMA spectrometer at the ISIS spallation neutron source, UK. This spectrometer is an indirect-geometry time-of-flight instrument for the study of coherent excitations in single crystals [14]. However, the data reported here were taken using the spectrometer in its diffraction mode rather than its inelastic scattering mode. The measurements were performed using a single ^{3}He detector which viewed the sample directly without an analyser crystal. The time-of-flight scan performed using this detector then corresponds to a measurement along a radial path in reciprocal space.

It is possible, using this time-of-flight technique, to measure rapidly whole regions of reciprocal space. This is done by stepping the rotation angle of the crystal, and at each step measuring a radial path via a time-of-flight scan which can then be used to construct a contour map of the intensity in that particular region of reciprocal space. Here measurements around the (001) and (111) Bragg peak positions are reported. All of the measurements were performed with the detector at a fixed scattering angle (2θ) of 60°. For the measurements around the (001) position, neutrons in the energy range from 8.3 to 11.4 meV were used, while in the vicinity of (111) neutrons of energy 25.4 to 32.0 meV were used. There is no soller collimation in the incident beam on PRISMA; however, the collimation due to

distance [15] is 0.25° between moderator and sample. Between sample and detector the soller collimation was 0.5°. An important feature of the time-of-flight diffraction technique is that it is free of the λ/n contamination problem encountered with a monochromatic beam at a steady-state source, and therefore a pyrolytic graphite filter is not required. Since we have scanned only a small portion of reciprocal space, it is not possible to state that there has not been a more dramatic change in magnetic structure than would be expected at the ICSDW–CSDW transition, whose energetics is dominated by Fermi surface nesting [2, 6], but the data obtained suggest that this is most unlikely.

Table 1. Start (T_s) and finish (T_f) transformation temperatures, and enthalpy (ΔH) and entropy (ΔS) changes for the ICSDW–CSDW transition in the Cr + 0.3 at.% Ru alloy crystal.

Run	T_s (K)	T_f (K)	ΔH (J mol^{-1}) (error: ±0.35)	ΔS (J mol^{-1} K^{-1}) (error: ±0.0023)
Cooling 1	248	234	−5.42	−0.0229
Heating 1	251	267	+ 5.89	+ 0.0229
Cooling 2	249	232	−5.74	−0.0240
Heating 2	252	266	+ 5.37	+ 0.0214
Cooling 3	250	233	−6.15	−0.0256
Heating 3	249	266	+ 5.22	+ 0.0203

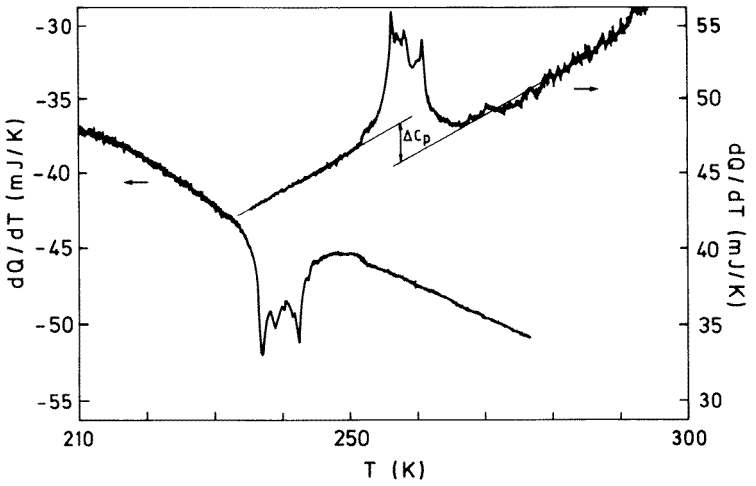

Figure 1. Thermal curves obtained during heating (upper curve) and cooling (lower curve) cycles for Cr + 0.3 at.% Ru alloy taken through the ICSDW–CSDW phase transition.

3. Calorimetric study of the CSDW–ICSDW phase transition

A typical, and reproducible, example of the thermal curve measured through the CSDW–ICSDW phase transition as the Cr + 0.3 at.% Ru alloy undergoes a heating and cooling run is shown in figure 1. The temperature range was chosen to be sufficiently wide to ensure that the transition was complete. Important features showing up from these curves are as follows.

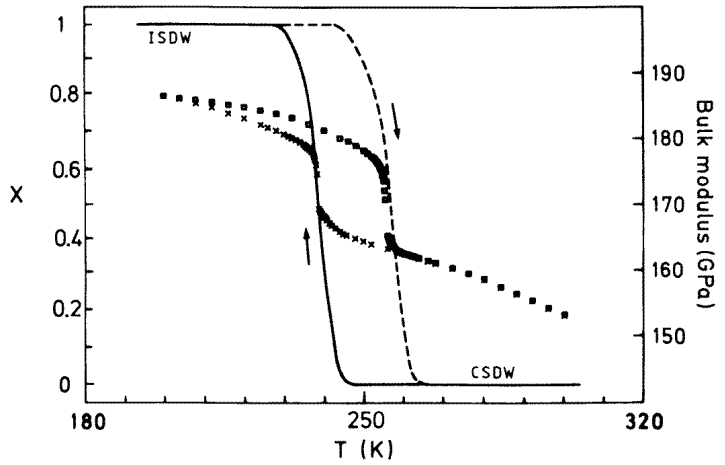

Figure 2. Temperature dependences of the fraction ($x(T)$) of Cr+0.3 at.% Ru alloy transformed from the ICSDW into the CSDW phase. The solid line corresponds to cooling and the dashed one to warming. Also included is the bulk modulus measured during a cooling (crosses) and heating (squares) cycle of the same crystal obtained from ultrasonic wave velocity measurements [10].

(i) The transition does not take place at a fixed temperature but is spread over several degrees. In table 1 the values of the starting (T_s) and finishing (T_f) temperatures for the forward and reverse transformations are listed. These temperatures T_s and T_f are similar, within experimental error, to those at which a steep change in ultrasonic wave velocity was found previously [10].

(ii) The transition exhibits thermal hysteresis. This confirms the conclusion drawn from the ultrasonic experiments that it has a first-order character [10]. A convenient way to display thermal hysteresis is to plot the transformed fraction ($x(T)$) against temperature, as shown in figure 2 (solid and dashed lines) together with measurements of the bulk modulus (crosses and squares) taken from reference [10]; the two sets of measurements correlate well. The transformed fraction ($x(T)$) at a given temperature T is obtained by taking advantage of the fact that the entropy is an extensive property; therefore:

$$x(T) = \frac{1}{\Delta S}\int_{T_s}^{T}\left(\frac{1}{T}\right)\left(\frac{\mathrm{d}Q}{\mathrm{d}t}\right)\dot{T}^{-1}\,\mathrm{d}T. \tag{3}$$

From figure 2 a reasonable agreement between calorimetric and ultrasonic measurements can be seen. The width of the $x(T)$ versus T loop at $x(T)$ equal to 0.5 is a useful quantitative measure of the thermal hysteresis. For this Cr + 0.3 at.% Ru alloy crystal this value is found to be 18 K.

(iii) The thermal curve does not appear as a smooth single peak but shows several peaks: the transition does not proceed smoothly and continuously (figure 1).

(iv) The heating curve shows a small discontinuity ΔC_P between the levels of the $\mathrm{d}Q/\mathrm{d}T$ curve before and after the transition (figure 1); the effect is not so clear in the cooling curve. Evaluation of this step in the calorimetric base-line enables determination of the difference in specific heat between the ICSDW and the CSDW phases. This difference is rather small, close to the limit of detectability of the measuring system, and therefore is subject to a substantial experimental error. The measured difference ($C_P^I - C_P^C$) between the specific heat C_P^I of the incommensurate phase and that, C_P^C, of the commensurate phase

is equal to 0.20 ± 0.14 J mol^{-1} K^{-1}. As Cr is an itinerant antiferromagnet, the magnetic contribution to its specific heat should be small. At 300 K ($T_N = 312$ K) the magnetic contribution in the ICSDW phase, estimated from data in reference [16], is only about 0.2 J mol^{-1} K^{-1}. After all, the magnetic states of the ICSDW and CSDW phases do not differ much; only the Q-vectors differ slightly.

The latent heat ΔH and the entropy change ΔS of the transition have been calculated (table 1). The values for forward and reverse transformations are coincident within the experimental uncertainty. The average values for the latent heat and the entropy change are $|\Delta H| = 5.6 \pm 0.5$ J mol^{-1} and $|\Delta S| = 0.023 \pm 0.003$ J mol^{-1} K^{-1} respectively. Latent heat and entropy changes have previously been determined at the CSDW–ICSDW transition in dilute Cr alloys for Cr–Mn [17], Cr–Fe and Cr–Si [18] alloys. The values found for Cr + 0.3 at.% Ru alloy are very similar to those reported for Cr–Mn alloys ($\Delta H = 5.8$ and 4.5 J mol^{-1} and $\Delta S = 0.028$ and 0.026 J mol^{-1} K^{-1} for Cr + 0.45 at.% Mn and Cr + 0.70 at.% Mn respectively [17]). For Cr–Si ($\Delta H = 0.3$ J mol^{-1} [17]) and Cr–Fe ($\Delta H = 0.4$ J mol^{-1} [18]) alloys, the measured latent heats are an order of magnitude smaller and correspond to a very small entropy change ($\Delta S \approx 0.002$ J mol^{-1} K^{-1}) at the transition. Furthermore for these two alloys, the kinetics of the CSDW–ICSDW transition, for which the thermal curve shows just a single peak, is different from that of the Cr + 0.3 at.% Ru and Cr–Mn alloys. It is interesting to note that the ΔH values obtained for the Cr + 0.3 at.% Ru and Cr–Mn alloys are close to that ($\Delta H = 4.8$ J mol^{-1}) measured for the latent heat at the CSDW–ICSDW transition for CuO [19]. In general the values found for ΔH and ΔS at CSDW–ICSDW transitions are very small in comparison to those of many solid–solid phase transitions: these ICSDW–CSDW transitions have only weak first-order character.

The pressure dependence measurements of the transition temperature for the same Cr + 0.3 at.% Ru crystal [10] enable us to make a comparative calculation of the latent heat, using the Clausius–Clapeyron equation, and in turn the entropy change as $\Delta S = -0.037$ J mol^{-1} K^{-1} in the direction of the CSDW–ICSDW transition and $\Delta S = +0.031$ J mol^{-1} K^{-1} for the CSDW–ICSDW transition. These values are slightly larger than the more direct calorimetric values obtained here. This seems to be a common feature since use of the pressure dependence of the transition temperature data also gives larger values than calorimetric ones for Cr + 0.45% Mn and Cr + 0.70% Mn [17].

4. Neutron diffraction study of monocrystalline Cr + 0.3 at.% Ru alloy traversing the CSDW–ICSDW transition

The neutron diffraction results obtained here for temperatures above 235 K are in agreement with and extend those of Boshoff *et al* [11]. There is a single magnetic Bragg peak at the (001) and equivalent positions, which corresponds to a commensurate antiferromagnetic structure. For the bcc structure Bragg peaks with $h + k + l =$ odd are forbidden for nuclear scattering from the crystal lattice, and consequently the (001) and (111) Bragg peaks arise from purely magnetic scattering. For temperatures below 235 K we observe the appearance of satellite Bragg peaks at the positions $(0, 0, 1 \pm \delta)$ and for temperatures below 215 K the disappearance of the commensurate Bragg peak at (001). With the crystal mounted with the $[1\bar{1}0]$ axis vertical, scattering from the satellites at $(0, 0 \pm \delta, 1)$ and $(0 \pm \delta, 0, 1)$, which are out of the equatorial plane, does not fall on the commensurate Bragg peak position, but at a distance $\delta/\sqrt{2}$ either side. A contour map of the intensity around the (001) Bragg peak position at a temperature of 125 K is shown in figure 3(a). The $(0, 0, 1 \pm \delta)$ satellite can be seen above and below the commensurate position at (001) well resolved from the scattering from the out-of-plane satellites on either side. Data extracted along the direction

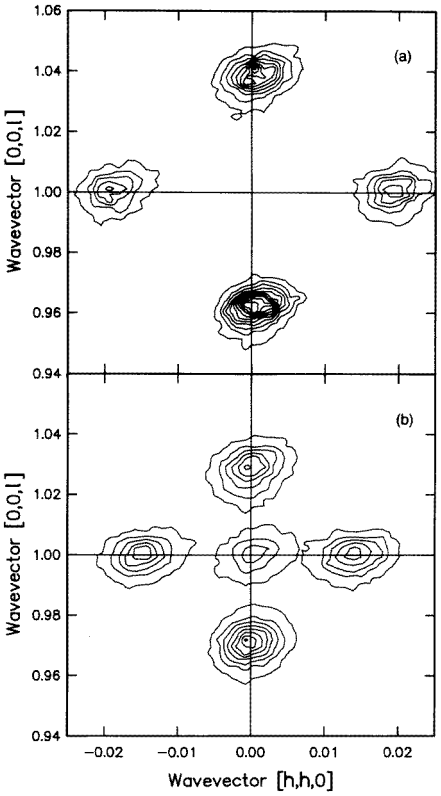

Figure 3. Contour plots of the elastic scattering intensities in the (*hhl*) plane in the vicinity of the (001) reciprocal-lattice point at (a) 125 K and (b) 225 K after warming from the ICSDW phase.

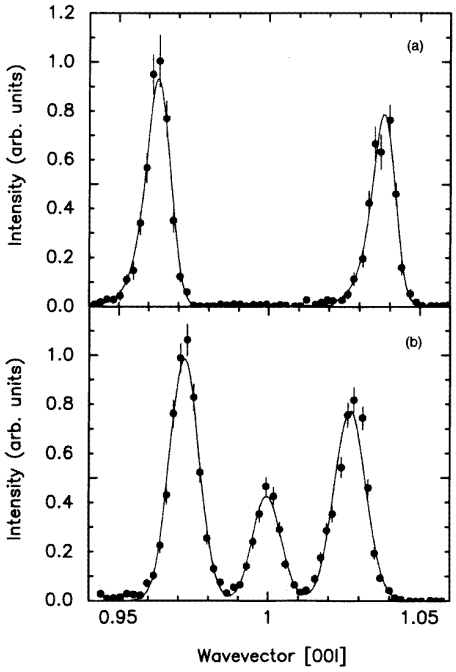

Figure 4. Scattering intensity along [001] across (001) at (a) 125 K and (b) at 225 K.

[001] passing through the (001) position, from this set of results, are shown in figure 4(a). The peaks at $(0, 0, 1 \pm \delta)$ in figure 4(a) correspond to those found in pure chromium and also to the satellites observed by Boshoff *et al* [11] in Cr + 0.3 at.% Ru.

The evolution with temperature on cooling of the heights of the satellites and the commensurate peak are summarized in figure 5 with the development of δ in the region of the transition shown in the inset. We see on cooling (figure 5) that the intensity of the commensurate peak starts to fall at approximately 232 K, with the satellites becoming visible at 234 K. At 216 K, the CSDW–ICSDW transition appears to be complete as the satellite peak heights reach a plateau and the scattering at the commensurate peak position becomes immeasurably small. Data collected on warming show that these transition temperatures differ somewhat from those observed by ultrasonic measurements [10]. The temperature dependence of the attenuation for each ultrasonic mode is characterized by a spike-like peak centred at T_{CI} (=238.8 K) on cooling and T_{IC} (=255.6 K) on warming, Although the crystal used for these neutron studies is nominally of the same composition as that used by Cankurtaran *et al* [10], a small difference between Ru concentration is highly likely within the error range of the electron microprobe analysis and given the small doping level, and would explain the difference in transition temperatures between the neutron scattering and ultrasonic data. Inspection of the phase diagram [20] indicates that the slope of the

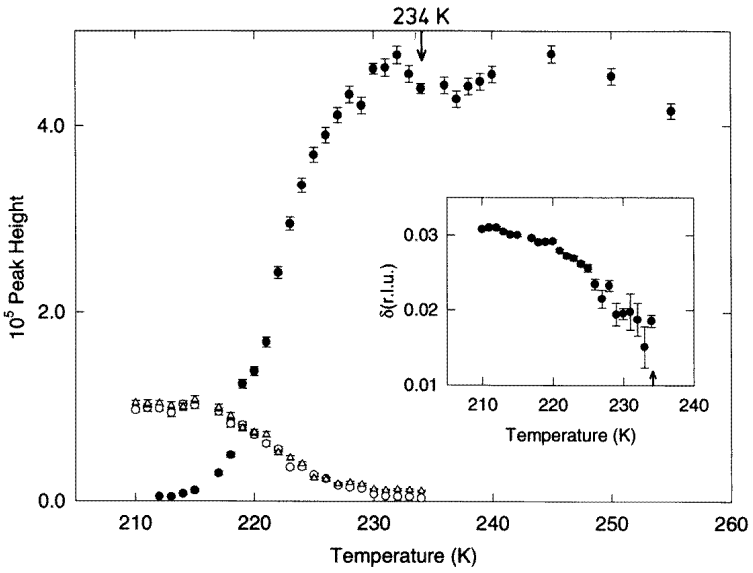

Figure 5. Scattering intensities of the (001) commensurate peak (●) and the satellite peaks (○, △) versus temperature on cooling. Inset: the thermal evolution of δ calculated from the positions of the satellite peaks.

composition dependence of the CSDW–ICSDW transition is about -0.6×10^3 K/at.% Ru: a compositional variation of only 0.02 at.% Ru would cause a 12 K change.

An interesting feature of the results shown figure 5 is that there is a region of approximately 28 K where the commensurate and satellite peaks all coexist, albeit with rapidly changing intensity. Over this temperature range the incommensurability parameter, δ (figure 5, inset), is increasing continuously from an initial value of approximately 0.015 r.l.u to a final value of approximately 0.03 r.l.u.

A scan across the (001) Bragg peak at 225 K after warming from the ICSDW phase (figure 3(b)) demonstrates the coexistence of magnetic satellites and a peak at the commensurate position. Figure 4(b) shows a cut made along the [001] direction passing through (001) extracted from this data set. On cooling toward the transition a reduction in the intensity of the commensurate peak of approximately 10% is observed at 238 K. The peak then recovers its previous intensity immediately prior to the transition. This dip coincides with the first observation of the satellite peaks on cooling. We note that the widths of both the satellite and the commensurate peaks through the transition do not display any unusual behaviour.

5. Conclusions

Calorimetric and time-of-flight neutron diffraction experiments have provided details of thermodynamic parameters and structural features of a Cr + 0.3 at.% Ru alloy crystal as it undergoes a commensurate and the incommensurate spin-density-wave phase transition, which can be summarized as follows.

(1) The first-order nature of the transition plays an important role in both the heat capacity and structural characteristics in the vicinity of the transition.

(2) The latent heat ($|\Delta H| = 5.6 \pm 0.5$ J mol^{-1}) and entropy ($|\Delta S| = 0.023 \pm 0.003$ J mol^{-1} K^{-1}) changes at the CSDW–ICSDW transition in Cr + 0.3 at.% Ru alloy are small: the transition is weakly first order. The results obtained by this direct calorimetric method are somewhat smaller than those determined by the indirect method using the Clausius–Clapeyron equation from pressure dependence measurements of the transition temperature. The difference ($C_P^I - C_P^C$) between the specific heats of the incommensurate phase and that of the commensurate phase has been determined as 0.20 ± 0.14 J K^{-1} mol^{-1}.

(3) The neutron diffraction experiments have shown that there is a temperature range of approximately 28 K in which the commensurate and the incommensurate peaks coexist. In this region the incommensuration factor δ is seen to increase until it achieves a value of approximately 0.03 when the ICSDW phase is fully established. These findings support the view that the transition is only weakly first order. There is no associated broadening of either the commensurate peaks, or the satellites. The coexistence of ISDW/CSDW phases during the CSDW–ISDW phase transition has previously also been observed in neutron diffraction studies on other Cr alloys. Booth *et al* [21] observed coexistence of commensurate and incommensurate SDW peaks in a temperature range of up to 100 K near the CSDW–ISDW phase transition of the Cr–Ge dilute alloy system with the ISDW phase being the stable low-temperature phase, quite similar to what has been found for the Cr + 0.3 at.% Ru crystal of the present study. Mixed ISDW/CSDW phases near the CSDW–ISDW transition have also been observed in the Cr–Fe system [22]. A Cr alloy inevitably contains an inhomogeneous distribution of solute atoms to a certain extent, and the coexistence of the ISDW and CSDW phases in Cr–Fe was explained as being due to sample inhomogeneities. This may in part also be responsible for the coexistence of these two phases in the Cr + 0.3 at.% Ru crystal of the present study.

(4) The broad anomaly in the specific heat data has a width of approximately 7 K, considerably smaller than the 28 K region over which the commensurate peak and the satellites are observed to coexist. If one considers the transition to start as the commensurate peak starts to reduce in intensity, and to be complete at the point at which the intensities of the satellites stabilize, one is still left with a transition of approximately 14 K in width. This difference may be attributed to small differences in the Ru concentration between the two samples. Since the properties are sensitive to the Ru concentration and inhomogeneity, it would be necessary to make measurements in the same place on one single crystal to make a direct comparison of the different techniques, but that has not proved feasible.

Acknowledgments

We are grateful to the United Kingdom Engineering and Physical Sciences Research Council for the provision of neutron beam time at the ISIS Facility. Financial support from CICyT, Spain, is acknowledged (Project No MAT95-0504).

References

[1] Overhauser A W 1962 *Phys. Rev.* **128** 1437
[2] Lomer W M 1962 *Proc. Phys. Soc.* **80** 489
[3] Werner S A, Arrott A and Kendrick H 1967 *Phys. Rev.* **155** 528
[4] Fawcett E 1988 *Rev. Mod. Phys.* **60** 209
[5] Fawcett E, Alberts H L, Galkin V Yu, Noakes D R and Yakhmi J V 1994 *Rev. Mod. Phys.* **66** 39
[6] Koehler W C, Moon R M, Trego A L and Mackintosh A R 1966 *Phys. Rev.* **151** 405
[7] Falicov L M and Penn D R 1967 *Phys. Rev.* **158** 476
[8] Kulikov N I and Tugushev V V 1984 *Sov. Phys.–Usp.* **27** 954

[9] Papoular R, Debray D and Arajs S 1981 *J. Magn. Magn. Mater.* **24** 106
[10] Cankurtaran M, Saunders G A, Wang Q, Ford P J and Alberts H L 1992 *Phys. Rev.* B **46** 14 370
[11] Boshoff A H, Alberts H L, du Plessis P de V and Venter A M 1993 *J. Phys.: Condens. Matter* **5** 5353
[12] Guénin G, Macqueron J L, Mantel M, Auguet C, Cesari E, Manosa Ll, Planes A, Ortin J, Picornell C, Segui C and Torra V 1987 *Proc. ICOMAT-86* (Nara: The Japan Institute of Metals) p 794
[13] Mañosa Ll, Bou M, Calles C and Cirera A 1996 *Am. J. Phys.* **63** 283
[14] Steigenberger U, Hagen M, Caciuffo R, Petrillo C, Cilloco F and Sacchetti F 1982 *Nucl. Instrum. Methods* B **53** 87
[15] Hagen M and Steigenberger U 1992 *Nucl. Instrum. Methods* B **72** 239
[16] Williams I S, Gopal E S R and Street R 1979 *J. Phys. F: Met. Phys* **9** 431
[17] Geerken B M, Griessen R, Benediktsson G, Åström H U and van Dijk C 1982 *J. Phys. F: Met. Phys.* **12** 1603
[18] Benediktsson G, Hedman L, Astrom H U and Rao K V 1982 *J. Phys. F: Met. Phys* **12** 1439
[19] Loram J W, Mirza K A, Joyce C P and Osborne A J 1989 *Europhys. Lett.* **8** 263
[20] Sidek H A A, Cankurtaran M, Saunders G A, Ford P J and Alberts H L 1993 *Phys. Lett.* **172A** 387
[21] Booth J G, Costa M M R, Rodriguez-Carjaval J and Paixao J A 1992 *J. Magn. Magn. Mater.* **104–107** 735
[22] Tsunoda Y 1994 *J. Phys.: Condens. Matter* **6** 8513